Histology to μCT Data Matching Using Landmarks and a Density Biased RANSAC

Natalia Chicherova[1,2], Ketut Fundana[1], Bert Müller[2], and Philippe C. Cattin[1]

[1] Medical Image Analysis Center, University of Basel, Basel, Switzerland
[2] Biomaterials Science Center, University of Basel, Basel, Switzerland
natalia.chicherova@unibas.ch

Abstract. The fusion of information from different medical imaging techniques plays an important role in data analysis. Despite the many proposed registration algorithms the problem of registering 2D histological images to 3D CT or MR imaging data is still largely unsolved.

In this paper we propose a computationally efficient automatic approach to match 2D histological images to 3D micro Computed Tomography data. The landmark-based approach in combination with a density-driven RANSAC plane-fitting allows efficient localization of the histology images in the 3D data within less than four minutes (single-threaded MATLAB code) with an average accuracy of 0.25 mm for correct and 2.21 mm for mismatched slices. The approach managed to successfully localize 75% of the histology images in our database. The proposed algorithm is an important step towards solving the problem of registering 2D histology sections to 3D data fully automatically.

1 Introduction

Image registration is the art of automatically aligning or warping medical imaging data. Registered data allows a more in depth analysis of the probed tissues as different modalities often represent different physical properties important to better understand and interpret the data at hand. Many approaches have been proposed in the last decades for 2D-to-2D and 3D-to-3D registration of the same or even different modalities [11]. However, registering 2D histological images to 3D data is a largely unexplored problem.

The need for reasonable 2D histology to 3D data registration becomes more and more important with the availability of affordable micro Computed Tomography (μCT) devices with high spatial resolution and tissue contrast. Combining the functional information from histology with the structural imaging data of the μCT provides better insights in identifying anatomical features of hard and soft tissues.

Only few papers are insofar directly related to the research at hand as they describe the registration of histological sections to CT and MR data. Seise *et al.* [9] proposed an interactive registration of histological sections to CT in the context of radiofrequency ablation. However, this approach highly relied on manual intervention in the registration step as well as in segmentation. Sarve *et al.* [8]

P. Golland et al. (Eds.): MICCAI 2014, Part I, LNCS 8673, pp. 243–250, 2014.
© Springer International Publishing Switzerland 2014

registered histological images of bone implants with synchrotron radiation-based μCT data. Their algorithm was based on segmentation of the implant by thresholding, which is not possible in our datasets, as the implant material is hardly visible and highly assimilated in the jaw bone. Other approaches deal with the registration of histological sections with soft tissue such as in the prostate [7] or the human brain [6] where MRI is more useful than CT. An additional factor is that the acquired μCT or μMR imaging data is generally of large size, amounting up to several hundred megabytes of data. However, only very little research has been devoted to efficiently register these type of datasets [5].

Using images of histological cross sections poses additional challenges to the already ill-posed problem of image registration. First, the histology images are susceptible to uneven lighting (vignetting artifact) and different contrasts from staining. Second, the histological sections may suffer from severe non-rigid deformations originating from the cutting process. Moreover, the histological images generally show different contrasts as compared to the μCT or μMR data that must be handled appropriately. Lastly, the potentially non-uniform background of the histological cuts may lead to erroneous results in the registration process.

In this paper we propose a novel approach for automatic registration of 2D histological cross sections to 3D μCT scans. This fully automatic feature-based registration approach makes use of the scale- and rotation-invariant feature detector SURF[2] and a modified density-driven RANSAC[3] plane-fitting. The main advantage of our method is that it can detect corresponding slices under different angulation that often appears in histological sectioning experiments. Furthermore, the computation time of our algorithm is notably shorter than of manual registration. The latter is estimated at 8 hours per slice. Finally, it does not require insertion of any additional landmarks hence can be readily applied to numerous biological data, where auxiliary inclusions are impossible.

2 Method

An illustration of the algorithmic pipeline is depicted in the Fig. 1. First, we determine corresponding feature points between the histological image and each image in the μCT volumetric data and extract their associated coordinates. Then, based on these coordinates, we build a 3D point cloud, where the third dimension corresponds to the slice number in the μCT data. As the distribution of the matched points is higher in the plane that corresponds best to a given histological slice (see Fig. 1(middle)) the remaining step reduces to a robust plane fitting in a noisy point cloud.

2.1 Data Acquisition

The sample data used for this work [10] originates from a jaw bone volume augmentation after tooth extraction study. In total ten clinical patients were included in this study. Biopsies of the jaw bones were taken from 4 to 11 months after implantation. The inner diameter of the specimen tubes was around 3 mm

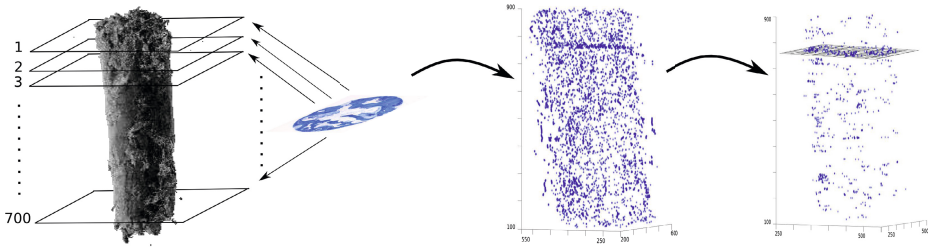

Fig. 1. Pipeline of the algorithm: (left) Feature matching of μCT data and histological image, (middle) 3D point cloud of matched points, (right) optimized RANSAC plane fitting

and the length was around 12 mm. The μCT of the whole specimen was acquired. Then five to nine histological cross-sections through the horizontal plane of the specimen were taken. Each histological slice (thickness 300 μm) resulted in an RGB image of size 2592×1944 pixels. The μCT data were 8 bit gray-scale 3D matrices with a range of data size $764 \times 764 \times (416 \div 1939)$ pixels, where the vertical axis corresponds to the third dimension. The corresponding resolution along vertical axis differed from 0.03 mm to 0.006 mm per slice.

2.2 Feature Detection and Matching

Let $I(x, y)$ and $V(x, y, z)$ denote the histological image and the μCT data volume accordingly, where z is associated with a slice number in the μCT dataset. Hence, $I : \Omega_I \subset R^2 \rightarrow R$ and $V : \Omega_V \subset R^3 \rightarrow R$. The rigid registration problem between these two modalities can be formulated as finding coefficients of the plane section in the μCT space that corresponds best to the histological image. In a first step we match each of the histological images to all axial μCT slices using a landmark-based approach. As a feature detection algorithm we rely on the scale- and rotation-invariant feature detector and descriptor SURF [2]. The choice of this detector is based on performed comparative analysis with SIFT[4]. We have found that SURF was more accurate and computationally efficient for our application. For a Matlab implementation of the SURF algorithm we used the opensource code by D. Kroon of Sep 2010[1], saving the default parameters. The number of octaves was set to 5, threshold to 0.0002. The main principal of this detector is based on scale-space extrema detection and stable feature localization. Applying the feature detector to an image, *e.g.* histological image I, we obtain a small subset of distinctive feature points $P(x, y) \subset I$. The descriptor vectors are then used for matching the feature points between the μCT and histological images. As the matching algorithm, we use the second-nearest-neighbor-criteria [4,1] that calculates the Euclidean distance between the descriptor vectors. A match is only accepted when the smallest Euclidean distance is less than 0.8

[1] `http://www.mathworks.ch/matlabcentral/fileexchange/28300-opensurf--including-image-warp-`

times the second smallest Euclidean distance. This process is then repeated for all the axial slices in the μCT dataset.

2.3 The 3D Feature Point Cloud

Suppose that the result of the above matching step is a set of feature points $P_z \subset V_z$ with coordinates (x_i, y_i), where $i = 1...\kappa_j$ and κ_j is the number of found matching feature points in a slice z. Having matched features for each of the N slices in the μCT volume will subsequently allow us to plot them as a point cloud, *i.e.* the 3D set of the keypoints $C = \{(x_{ij}, y_{ij}, z_j)\}$ $(j = 1...N)$ with the third dimension z representing the slice number in the μCT data, see Fig. 1(middle). Here, the total number of feature points for the whole μCT data is determined as $M = \sum_{j=1}^{N} \kappa_j$.

As one would expect, the resulting point cloud shows an increased density of found matches at the correct location of the histology section. This holds true even for histological images that are tilted with respect to the z-axis of the μCT dataset. This plane - well visible in the point cloud of Fig. 1(middle) - corresponds to the best position for the histological slice. In order to efficiently extract the plane parameters, we define a binary matrix $B(x, y, z) : \Omega_V \subset R^3 \rightarrow R$ as

$$B(x, y, z) = \begin{cases} 1 & \text{if } (x, y, z) \in C \\ 0 & \text{otherwise,} \end{cases}$$

which is then convolved with a 3D Gaussian as $B_\sigma = G_\sigma * B$. Thus, in each point we obtain a new intensity value that is influenced by the neighboring keypoint distribution across the μCT space and thus reflects the local density of matched points.

2.4 Density-Driven RANSAC for Robust Plane Fitting

One of the most widely used robust algorithms for extracting shapes from a data set with outliers is RANSAC [3]. The algorithm randomly selects a minimum number of points that uniquely defines a fitting shape. Then the corresponding primitive is constructed. In our problem, the model of interest is a plane $Ax + By + Cz + D = 0$ and the minimum number of points is 3. Therefore, the output parameter of the algorithm is a four dimensional normal vector $\boldsymbol{n} = [A\, B\, C\, D]^T$. RANSAC then counts the number of points within the distance threshold t to the obtained candidate model (inliers). If the number of inliers for one model is larger than in the previous iteration, the new model parameters are retained. Otherwise, another subset is randomly selected. Depending on the ratio of inliers over outliers, this process has to be repeated multiple times to assure with a high probability that a solution is found when present. The large amount of outliers in our data would result in a large number of iterations.

In this work we thus propose to bias the random sampling of the RANSAC plane fitting process towards points with high density *i.e.* points that are close to the plane of interest. To optimize the plane detection algorithm, the dataset

B_σ is further reduced to $\rho < M$ points by retaining features with the largest density values. However, the new dataset $B_\rho \subset B_\sigma$ still contains some outliers due to high similarities within a specimen along the vertical axis.

To further reduce the number of required sampling iterations, we bias the random sampling code towards preferring points with a higher local density. Thus points with a high local density have a higher probability of being selected. Suppose that each density value of the dataset B_ρ is assigned to the weighting vector $\mathbf{w} = \{w_l\}$, where $l = 1...\rho$. Therefore, instead of using the unbiased classical sampling of the original RANSAC, the probability of picking an element $b_m \in B_\rho$ is then defined as $p_m{=}w_m/\sum_{l=1}^{\rho} w_i$.

A further optimization is associated with the angle α between the z-axis and the plane formed by the currently randomly sampled points from the dataset. Based on our observations we restrict this angle to lie between $-\alpha_{hist} < \alpha < \alpha_{hist}$. In other words, for every iteration, the 3D coordinates of the sampled points $\{b_1, b_2, b_3\} \in B_\rho$ are used to calculate the normal of the plane that goes through these points $\boldsymbol{n} = (b_2 - b_1) \times (b_3 - b_1)$. We then find the angle $\alpha = \arccos(n_z / \|\boldsymbol{n}\|)$, subject to $-\alpha_{hist} < \alpha < \alpha_{hist}$. Therefore, only planes that satisfy this constraint are considered for further procession in RANSAC. These two modifications allow to robustly fit a plane to the selected points and to obtain its parameters. An example of the point cloud with corresponding plane fit is shown in the Fig. 1.

Finally, we make a cut through the μCT data matrix along the fitted plane. The image in this cut is the result of our algorithm and should be maximally similar to the histological image.

Algorithm 1. 2D-3D matching

Input: Histological image I and μCT 3D dataset V, RANSAC threshold t=10, ρ=1000, $\alpha_{hist} = \frac{\pi}{8}$
Output: Plane parameters $\boldsymbol{n}$

```
Convert I to gray scale
for all V_j, (j = 1...N) do                ▷ Detect coordinates of matching points
    (x_i, y_i) = SURF(I, V_j)
    Build 3D set of coordinates C = {(x_ij, y_ij, z_j)}
end for
Create a binary 3D matrix B(x, y, z)
for (x, y, z) ∈ B do
    if (x, y, z) ∈ C then
        set B(x, y, z) to 1
    end if
end for
Convolve with Gaussian: B_σ = G_σ * B
Find ρ highest values in B_σ
Define B_ρ ⊂ B_σ, i.e. keep ρ points with the highest values
n=RANSAC(B_ρ,t,α_hist, w)        ▷ Fit a plane into B_ρ using its values as weights w
return n
```

3 Results

Our framework was validated on ten μCT datasets with overall 60 histological cross section images. For each histological slice we obtained a four dimensional vector which uniquely describes a plane in a 3D space. To compare the automatically found results with manually found locations we estimated the z-coordinate along the μCT volume and the angle between z-axis and the normal to the plane which represents a cut of the specimen. The z-coordinate was calculated as a center point of the obtained plane. All manually found matching parameters were obtained from VG studio which provides a four-dimensional vector of the searching plane and automatically computes the center point of the plane, *i.e.*, z-coordinate. We also performed a visual assessment of the automatically found images. In Fig. 2, we showed two examples of a matched slice found automatically ((a) and (d)) in comparison with manually found ((b) and (e)) and histological image ((c) and (f)). The complete result of the visual estimation with corresponding comparison with the ground truth values is summarized in Table 1. In nine out of ten datasets our approach has allocated at least half of the histological slices with an average difference of 0.25 mm. For the datasets 4, 5 and 10 the algorithm showed poor performance. The average distance for mismatched slices averaged around 286 slices and an overall accuracy for mismatched slices reached 2.21 mm. This might be due to high intensity variations within the μCT dataset and the inhomogeneous dying of the histological slices (see Fig. 3(a)). The extrema detector was very sensitive to intensity changes and dirt spots on the histological slices. This caused wrong feature responses and consequently incorrectly matched images.

The comparison of the angles with the ground truth is shown in Table 2. For intuitive reasons, we provided negative angles instead of angles around 360° to stress small alternation of the cutting section slopes. For small angles (around 5°) our approach showed high efficiency, whereas, for the angles of more than 10°, which corresponded to 0.53 mm of the specimen, it often found only a close approximation to the desired section of the μCT volume. For example, for the dataset 10, it has found a very close slice number, but determined a wrong angulation.

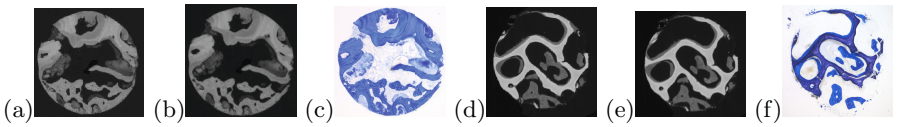

Fig. 2. (a),(d) Automatically found image. (b),(e) Manually found image. (c),(f) Histological image.

Table 1. Number of matched and mismatched images with corresponding average differences between automatically and manually found slices

Data set	1	2	3	4	5	6	7	8	9	10
Number of Matched slices	6	9	6	1	3	5	5	3	3	3
Average distance [mm]	0.06	0.04	0.9	0.17	0.05	0.59	0.24	0.07	0.16	0.13
Average difference [slices]	10	3	8	6	3	63	10	4	10	9
Number of Mismatched slices	0	0	1	4	3	1	1	1	2	3
Average distance [mm]	-	-	0.17	2.71	4.56	2.96	1.07	0.67	0.76	1.37
Average distance [slices]	-	-	15	94	286	314	45	40	47	91

*Note that number of slices per 1 mm is different for different samples.

Table 2. Comparison of average automatically found angles for matched slices with manually found angles

Data set	1	2	3	4	5	6	7	8	9	10
Average automatic angle [°]	1	1	1	-23	4	-1	-4	5	5	19
Manual angles [°]	-2	-5	5	-22	4	-19	-7	19	-8	-13

4 Discussion

Our novel algorithm for automatic 2D-3D registration showed a very high efficiency and small computational complexity and can be readily applied to the matching problem.

However, it has certain limitations regarding the feature detection step. Despite the good feature matching performance of SURF for most images it can not be considered a multi-modal approach but rather one that is robust against lightning changes. This also explains its poor performance when matching histological sections with non-uniform intensity variations. Moreover, additional complication arose from the histological slices that were compiled from disintegrated pieces (see Fig. 3(b)) and could not be readily matched with the same specimen. To overcome these limitations we want, firstly, to focus on developing a feature detector and descriptor that better will account for these specific characteristics and will efficiently work for multi-modal 2D-3D registration. Secondly, we want to include a non-rigid deformation estimation once the initial plane has been found. Lastly, we plan on further speeding up the calculation time by parallelization and GPU implementations. With a computation time of less than four minutes on a single-threaded MATLAB implementation, the algorithm still leaves room for further optimization and parallelization. This is irrespective of any angulation between the histology sections with respect to the μCT data.

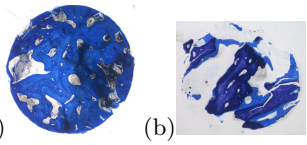

Fig. 3. (a) Inhomogeneous dying of the histological slice from the 5th dataset. (b) Compiled from pieces histological slice from the 8th dataset.

Acknowledgements. We would like to thank members of Biomaterials Science Center (University of Basel): Anja Stalder for the manually found slices and Simone Hieber for the help with the project. The work is funded by SNSF (project 150164).

References

1. Baumberg, A.: Reliable feature matching across widely separated views. In: IEEE Conference on Computer Vision and Pattern Recognition, vol. 1, pp. 774–781 (2000)
2. Bay, H., Ess, A., Tuytelaars, T., Van Gool, L.: Speeded-up robust features (SURF). Computer Vision and Image Understanding 110, 346–359 (2008)
3. Fischler, M.A., Bolles, R.C.: Random sample consensus: a paradigm for model fitting with applications to image analysis and automated cartography. Communications of the ACM 24, 381–395 (1981)
4. Lowe, D.G.: Distinctive image features from scale-invariant keypoints. International Journal of Computer Vision 60, 91–110 (2004)
5. Mosaliganti, K., Pan, T., Sharp, R., Ridgway, R., Iyengar, S., Gulacy, A., Wenzel, P., de Bruin, A., Machiraju, R., Huang, K., et al.: Registration and 3D visualization of large microscopy images. In: SPIE Medical Imaging, vol. 6144 (2006)
6. Osechinskiy, S., Kruggel, F.: Slice-to-volume nonrigid registration of histological sections to MR images of the human brain. Anatomy Research International (2010)
7. Ou, Y., Shen, D., Feldman, M., Tomaszewski, J., Davatzikos, C.: Non-rigid registration between histological and MR images of the prostate: A joint segmentation and registration framework. In: IEEE Computer Vision and Pattern Recognition Workshops, pp. 125–132 (2009)
8. Sarve, H., Lindblad, J., Johansson, C.B.: Registration of 2D histological images of bone implants with 3D SRμCT volumes. In: Advances in Visual Computing, pp. 1071–1080 (2008)
9. Seise, M., Alhonnoro, T., Kolesnik, M.: Interactive registration of 2D histology and 3D CT data for assessment of radiofrequency ablation treatment. Journal of Pathology Informatics 2, 72 (2011)
10. Stalder, A.K., Ilgenstein, B., Chicherova, N., Deyhle, H., Beckmann, F., Müller, B., Hieber, S.E.: Combined use of micro computed tomography and histology to evaluate the regenerative capacity of bone grafting materials. International Journal of Materials Research (2014)
11. Zitova, B., Flusser, J.: Image registration methods: a survey. Image and Vision Computing 21, 977–1000 (2003)